Quaternary Science Reviews 29 (2010) 913–927

Contents lists available at ScienceDirect

Quaternary Science Reviews

journal homepage: www.elsevier.com/locate/quascirev

Sedimentary evidence of landscape and climate history since the end of MIS 3 in the Krkonoše Mountains, Czech Republic

Zbyněk Engel [a,*], Daniel Nývlt [b], Marek Křížek [a], Václav Treml [a], Vlasta Jankovská [c], Lenka Lisá [d]

[a] Department of Physical Geography and Geoecology, Charles University in Prague, Albertov 6, 12843 Praha, Czech Republic
[b] Czech Geological Survey, Leitnerova 22, 65869 Brno, Czech Republic
[c] Botanical Institute, Czech Academy of Sciences, Poříčí 3b, 60300 Brno, Czech Republic
[d] Geological Institute, Czech Academy of Sciences, Rozvojová 269, 16502 Praha, Czech Republic

ARTICLE INFO

Article history:
Received 20 December 2008
Received in revised form
3 December 2009
Accepted 10 December 2009

ABSTRACT

A sedimentary core recovered from the cirque basin of Labský důl valley (1039 m a.s.l.) in the Krkonoše Mountains reflects the environmental history for approximately the last 30,000 years. Analyses of magnetic susceptibility, carbon content, pollen assemblages and macrofossil data in a 15 m thick sediment sequence provide the first continuous record of Lateglacial and Holocene vegetation history in Sudetes region of the Czech Republic. The succession of sedimentary units in the lower part of the core suggests that the cirque was ice-free before the onset of the last glaciation at the beginning of marine isotope stage 2. Highly variable climate prevailed during this period with cold conditions culminating about 18 cal ka BP. Cold climates persisted until the Lateglacial period, evidenced by an identified warming and subsequent cooling event correlated with the Younger Dryas period. Sparse, treeless vegetation dominated in the catchment area at that time. The sequence of interrupted thinly laminated silts reflects the retreat and temporary readvance of a local glacier in the cirque during 12.5–10.8 cal ka BP. Subsequently, the alpine treeline ecotone gradually shifted above the cirque floor. Palaeoclimatic conditions in the early Holocene fluctuated strongly, whereas since 5.1 cal ka BP conditions have been more stable. Pollen-based climate reconstructions suggest significant cooling at around 9.8–9.3, 7.7–7.5 and 4.0–3.3 cal ka BP. Spruce forests have dominated the site since 5.0 cal ka BP when the vegetation became similar to the modern one. Two phases of increased sedimentation were identified within the Holocene culminating about 9.2–7.5 cal ka BP and 5.8–5.5 cal ka BP. Sediment yield was as high as 2.4 mm yr^{-1} during the period, reflecting environmental changes during the Atlantic/Sub-Boreal transition.

1. Introduction

The Krkonoše Mountains belong to the Hercynian ranges in Central Europe. They are located within an ice-free zone between the Scandinavian ice sheets and the glaciated area of the Alps during the Quaternary. Within glacial periods, small mountain glaciers developed in several valleys in the central part of the Krkonoše Mts, leaving landform and sedimentary evidence of climate changes in the landscape. Since mountain environments generally lack a sufficient sedimentary record this evidence is highly significant for establishing local stratigraphy. In this respect, the upper Labe valley in the Krkonoše Mts is very important because it belongs to a few mid-mountain areas in the continental Europe with well-preserved glacial record and organic deposits rich in palaeoecological evidence (Carr et al., 2007).

The evidence from the Krkonoše Mts suggests that the climate was very cold and continental during the late Weichselian (Traczyk, 2004). Mean annual temperature in the summit area was close to the range of −8 to −10 °C according to the periglacial evidence (Chmal and Traczyk, 1993). During the marine isotope stage (MIS) 2 the amount of precipitation was substantially lower than at present, reaching about 500–700 mm (Czudek, 2005). Predominantly westerly winds prevailed in the region, influencing the distribution of snowfields and glaciers in leeward sides of high-elevated summit plateaus (Migoń, 1999).

The existence of thick weathering mantles, continuous permafrost and intense frost action generated through a variety of periglacial processes dominated the landscape evolution (Jahn, 1977). At least 11 valley heads have been identified to have contained former local mountain glaciers (Engel, 1997). The largest of them have

* Corresponding author. Tel.: +420 22 195 1373; fax: +420 22 195 1367.
E-mail address: engel@natur.cuni.cz (Z. Engel).

0277-3791/$ – see front matter © 2009 Elsevier Ltd. All rights reserved.
doi:10.1016/j.quascirev.2009.12.008

accumulated multiple series of moraines in the valleys of the upper Labe, Úpa and Łomnica rivers and in front of the Śnieżne Kotły Cirques. Evidence of ^{10}Be exposure ages reported by Braucher et al. (2006) combined with Schmidt-hammer data from the upper Labe and Úpa valleys (Carr et al., 2007) suggest that all preserved moraines accumulated during the Weichselian glaciation and that glacier have retreated since 14 ka BP (Engel, 2007). However, these data provide little evidence for deglaciation chronology and the age of moraines in other valleys. With the rapid amelioration of the climate in the Lateglacial period caused the glaciers and permafrost to decay, periglacial processes and aeolian activity weakened (Chmal and Traczyk, 1998). Two phases of retrieved solifluction, glacier activity and frost-related processes were identified at the termination of the Lateglacial period (Traczyk, 2004). Sub-arctic to arctic tundra that prevailed in the Krkonoše Mts during the full glacial was gradually colonized by shrub and forest communities during the Lateglacial (Jankovská, 2007).

The temperature and precipitation increased substantially at the beginning of the Holocene in Central Europe and humid climate persisted over the Early Atlantic period (Rybníčková and Rybníček, 2001). The Middle Atlantic is considered to be the most humid period in the Holocene whereas dry and humid oscillations predominated in the Late Atlantic (Ložek, 2007). Due to a general warming trend at the early Holocene, permafrost and relics of local mountain glaciers thawed. The evidence from the upper Labe and Łomnica valleys suggests that local glaciers were in the state of advanced decay as early as 10 ka ago and only small relics of glaciers may have survived attached to cirque headwalls (Chmal and Traczyk, 1998; Mercier et al., 2000). As a consequence of increased precipitation in the Atlantic period, the erosion of rivers increased and the coarser material was frequently delivered to the foreland of the mountains during this time (Chmal and Traczyk, 1998). The Lateglacial tundra vegetation was gradually replaced by pine and birch dominated forest which expanded up to 1450 m elevation during the Atlantic period (Treml et al., 2006). The development of raised bogs started on the summit plateaus in the Atlantic period (Hüttemann and Bortenschlager, 1987).

The Krkonoše Mts experienced a substantial cooling during the Sub-Boreal period (Jankovská, 2004). The average temperature of vegetation growth season in the Early Sub-Atlantic was 2 °C lower compared to the present time (Skrzypek et al., 2009). The cold climate and the increase of humidity can be traced throughout the Early Sub-Atlantic period with precipitation verging on the present level at the beginning of modern times (Ložek, 2007). The Sub-Boreal environment was characterized by the retrieve of slope processes and also by the sedimentation facilitated by the increased precipitation (Chmal and Traczyk, 1998). During the Sub-Atlantic period the rate of the slope and fluvial accumulation increased forming the lowermost floodplain terraces in larger valleys (Bieroński et al., 1992). The enhanced sediment supply was facilitated by deforestation and hillside ploughing, as was shown by Dumanowski et al. (1962). The retreat of forest and changes of its species composition reflect the Sub-Boreal climate shift as well as a rapid expansion of human activities since the Sub-Atlantic period (Jankovská, 2007).

This paper describes results of a multidisciplinary investigation of the most complete sedimentary record recovered in the Krkonoše Mts situated in the upper Labe valley (Fig. 1). A preliminary description of the sedimentary environment and a synopsis of the palaeoenvironmental conditions has already been published from this site (Engel et al., 2004; Jankovská, 2004), along with stable-isotope evidence (Engel et al., in press). In this paper we present results of detailed sedimentological and palaeoecological investigations applied to the core samples taken in 2006.

2. Regional setting

The Krkonoše Mts comprise high-elevated plateaus defined by WNW–ESE oriented ridges (Fig. 1). The main ridge (1400–1600 m a.s.l.) falls northward abruptly whereas the parallel southern ridge (1300–1500 m a.s.l.) verges into rounded ridges of N–S orientation that are separated by deep river valleys. Glacial geomorphology dominates the relief of the central part of the Krkonoše Mts where cirques and troughs are deeply incised into the summit plateaus. The best-developed cirques border the northern part of the summit plateaus which have acted as deflation surfaces supplying snow to the glaciers around (Migoń, 1999). The less-developed cirques are distributed along the eastern and southern borders of plateaus from where glaciers extended into the well-channelled valleys of the Labe and Úpa rivers transforming them into troughs.

The sampling site is located within the cirque of the upper Labe valley at 1039 m a.s.l. The cirque and the adjacent catchment area of the Labe River comprise of fine- and medium-grained biotitic granites of early Carboniferous age (Mazur and Aleksandrowski, 2001). The bottom of the cirque is covered with mire dominated by communities of *Sphagnum girgensohnii*, *Polytrichum commune*, *Eriophorum vaginatum* and *Juncus filiformis*. *Pinus mugo* and *Sorbus sudetica* are present in the transitional area between the mire and the cirque headwall whereas the southern margin of the cirque is covered by *Picea abies* forest. Although the site is situated almost 300 m below the treeline ecotone, it is connected with treeless summit areas through forest-free avalanche tracks.

The leeward position of the cirque affects the topoclimatic conditions in the sampling site. The mean annual temperature in the study area is about 2 °C. This is estimated from data collected during the years 1961–2000 at Labská bouda weather station (1310 m a.s.l.), located 1 km to NW from the study area. The mean annual precipitation at the station is about 1459 mm yr^{-1} (Metelka et al., 2007). Once in a few years or decades, heavy precipitation events occur with more than 100 mm of rainfall per day (Metelka et al., 2007). As the maximum water retention capacity of the soil profile in the Labe river headwater is low, intense precipitation events result in floods of the cirque floor.

3. Materials and methods

3.1. Material sampling

A core was drilled in the deepest place of the cirque basin (50°45′46″N, 15°33′8″E, 1039 m a.s.l.), located about 200 m above the confluence of the Labe and Pančava rivers (Fig. 1). An Eijkelkamp peat sampler was used for collecting the upper section of the sedimentary record down to 1300 cm whereas a percussion core sampler with a synthetic foil liner was applied to the lowermost sequence (1300–1505 cm). The peat sampler allows collecting of 50 cm long sections of uncompressed cores and a synthetic foil liner collects 1 m long sections. The upper 20 cm of the core contained fresh plant material and was sampled with a knife. The core-sections were divided into 2.5 cm slices. The slices were sub-sampled for particle-size analysis, clast morphology and micromorphology, total organic and inorganic carbon content, environmental magnetic susceptibility and pollen analyses. In total 17 samples were selected for radiocarbon dating: macroremains of *Sphagnum* (10 samples from 50–354 cm core section), plant macroremains (6 samples from 395 and 1040 cm depths) and bulk sample of laminated sediment (1 sample from 1487 cm). Material from two sequences (1300 and 1500 cm) was selected to derive an optically stimulated luminescence (OSL) age.

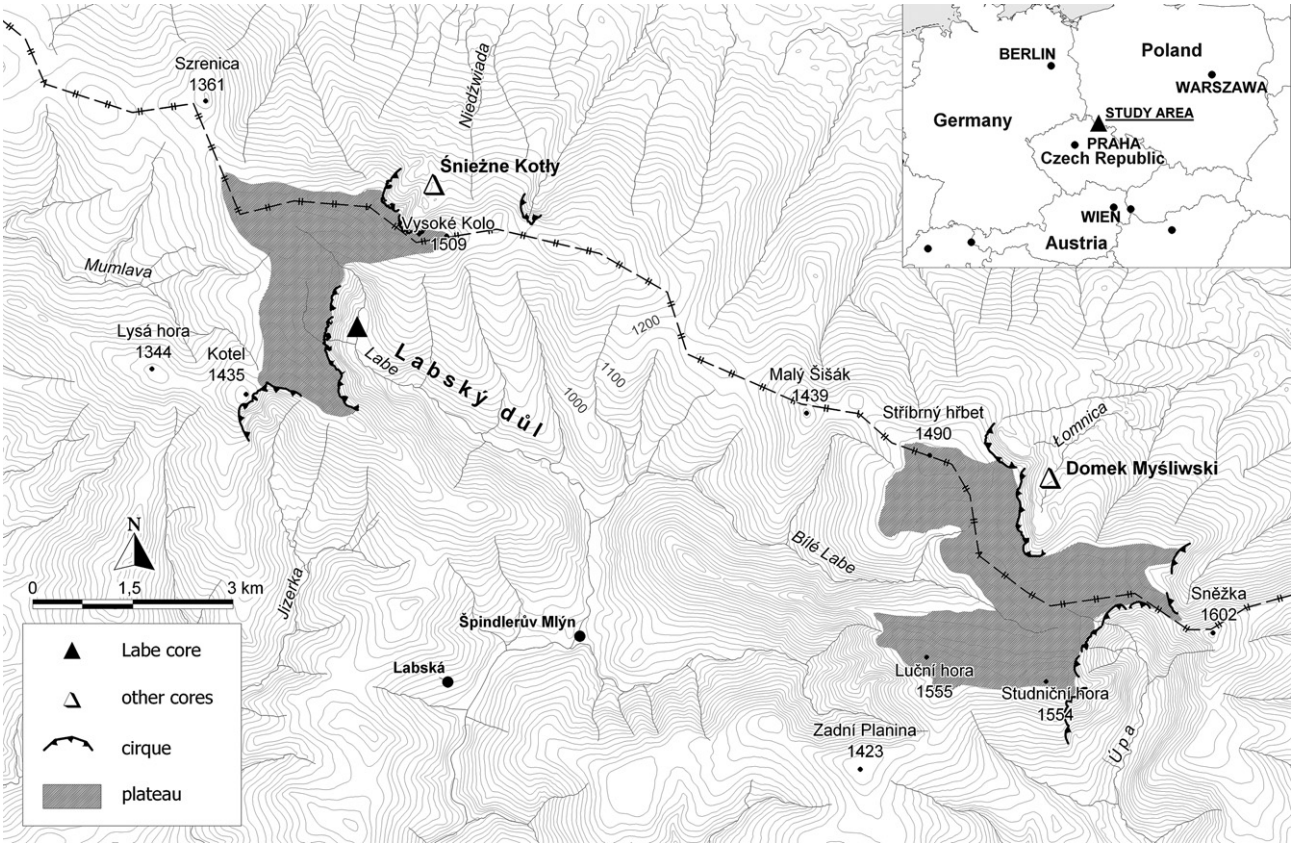

Fig. 1. Location of the upper Labe valley in the Krkonoše Mts, the Czech Republic. The solid triangle represents the position of the core described in this study.

3.2. Physical composition and pollen analyses of samples

The grain size was measured with combined sieving and laser diffraction methods to cover the wide size spectra. Dry sieving with Retsch AS 200 sieving machine covers the coarser grain fractions (4–0.5 mm) whereas Cilas 1064 laser diffraction granulometer was used for the finer ones (500–0.04 μm). Ultrasonic dispersion and distillate water were used prior to analyses in order to avoid flocculation of the particles. The sampling and laboratory analyses follow the methodology of Gale and Hoare (1991). The raw data were plotted on a histogram and a cumulative frequency curve which provided values for calculations of particle size parameters.

The sedimentary succession in the core has been divided into units defined by textural differences, colour changes and macrofossil content. These units have been labelled alphabetically in their ascending stratigraphic order. Sedimentary units which show grading in grain size or are interrupted by intervening units, are further divided into subunits. The validity of the macroscopic distinction of lithostratigraphic units is supported by the laboratory data which show that the visible changes coincide with marked changes in grain-size distribution and TC. Individual units are described by using the classifications of Folk (1954) for sorted unconsolidated sediments and non-genetic classification of Moncrieff (1989) for poorly sorted sediments. Colour of sediments was classified with a Munsell Soil Color Chart (2000).

The particle shape analysis was applied to the main sedimentary units. Long, intermediate and short axes of clasts were measured by using a vernier calliper. Individual measured values were displayed using the TRI-PLOT spreadsheet method of Graham and Midgley (2000). Ternary diagrams were used for presentation of the data. The morphology of quartz grains was studied in order to determine the mode of transport and post-depositional changes. Altogether 13 samples (50–70 grains of medium-grained sand) were treated by the following standard procedures and analysed by using the Cameca electron microscope; the atlas of grain surface morphology of Mahaney (2002) was used for evaluation. Micromorphological analysis of six thin sections recovered from units D and E followed the procedure outlined by Stoops (2003).

Total carbon (TC) content was analysed by using a CNS analyser. Inorganic carbon (TIC) content was measured as $CaCO_3$ with a Coulometer. Organic carbon (TOC) content was calculated as the difference between TC and TIC. Following the procedure described by Gale and Hoare (1991), samples were dried at 105 °C and combusted in an oven at 550 °C for 8 h. The results are expressed as percentage of dry weight.

Environmental magnetic susceptibility was measured as mass susceptibility (χ) in 10^{-9} m^3 kg^{-1} by using the KLY-4S Kappabridge. For further summary of magnetic parameters and terminology see Evans and Heller (2003).

Pollen analysis was applied to the material at a 10 cm interval (Moore et al., 1991). Additionally, algaeological and plant macroremains analyses were performed, since limnic deposits were identified within the section. All samples were treated with HF for 24–36 h and heated in 10% KOH. Subsequent acetolysis treatment removed the undesirable organic contaminants, particularly the cellulose. Pollen grains, spores and algae were identified and counted under ×400–1000 magnification. The data were processed using Tilia and Tilia Graph software (Grimm, 1991).

3.3. Radiocarbon and optically stimulated luminescence dating

Two dating methods were applied to samples from the core to achieve time-control for the sedimentary profile. Selected organic material was dated by using Accelerator Mass Spectrometry (AMS)

^{14}C method while single aliquot optical luminescence was applied to predominantly mineral sequences in the lower part of the core.

Seventeen samples from the profile were dated using AMS method at the Radiocarbon Laboratory of the University of Erlangen. The conventional ^{14}C ages were corrected for sample isotopic fractionation to a normalized value of $\delta^{13}C = -25‰$ and calibrated using the data set of the IntCal04 calibration curve and OxCal 4.0 program (Bronk Ramsey, 2001; Reimer et al., 2004). The only sample (from the depth 1487 cm) exceeding the range of the IntCal04 curve was calibrated using the CalPal-2007 Hulu data set and CalPal program (Weninger et al., 2007; Weninger and Jöris, 2008). Since no single value can adequately describe the shape of a calibrated radiocarbon probability density function, the full distribution was used (Telford et al., 2004). A single estimate was used to determine the rate of sedimentation only. In this case, the median of the probability distribution function was used to obtain a central estimate of the calibrated dates. The ^{14}C dates in this article refer to calibrated years before present (cal ka BP) where zero year is equal to 1950 AD. Radiocarbon dates in this paper are given rounded following the magnitude of the standard error (Stuiver and Polach, 1977). The age of sections between dated horizons was calculated proportionally for each sample pair. The chronostratigraphic subdivision of the Lateglacial and Holocene proposed by Mangerud et al. (1974) is referred with calibrated ages for its boundaries.

In order to obtain the age of an organic-poor sequence in the lowermost part of the core, coarse quartz grains extracted from two sections were dated using optically stimulated luminescence at the Sheffield Centre for International Drylands Research luminescence laboratory. As a part of the laboratory analyses, possible disturbance or incomplete reset of samples was assessed. Obtained OSL ages are quoted in years from the day of dating (2007) and are presented with one-sigma confidence intervals which incorporate systematic uncertainties and errors associated with dating procedures.

4. Results

4.1. ^{14}C-dates and OSL age

Calibrated and corrected radiocarbon dates obtained from 17 core samples are presented in Table 1. Fig. 2 shows the correlation between the calibrated age and depth of the corresponding core samples. The linear regression equation calculated for the 13 samples from the upper section (up to 500 cm depth) is different from the one calculated for the whole core. Since the uncertainty associated with the age calculation for the core sediments is highly dependent on the type of regression used, we have relied on calculating the age of the core samples by using the rate of sediment deposition between two successive radiocarbon dates.

Using calibrated age and depth values for adjacent dated sample pairs in the core, the mean sedimentation rates were calculated for 16 sections (Table 1). The mean sedimentation rate varies significantly in the core, ranging from 0.2 to 2.4 mm yr^{-1}. Judging from the stratigraphy, these variations are likely to be caused by changes in the rate of deposition and erosion during various time spans. The mean sedimentation rate ranges between 0.2 and 1.2 mm yr^{-1} in the upper part (0–290 cm) of the core which comprises mostly of *Sphagnum* peat. This suggests relatively calm accumulation of peat without significant erosion events since 5.5 cal ka BP. On the other hand, higher sedimentation rates occurred between 5.5 and 10.9 cal ka BP (290–963 cm) culminating at 5.5–5.6 cal ka BP (290–325 cm) and 7.5–9.2 cal ka BP (500–797 cm).

Table 2 provides a summary of optical luminescence dating. Amount of absorbed dose since the sample burial, dose rate and calculated age for samples Shfd06134 and Shfd06135 are presented. The results of sedimentary bleaching analyses showed that the sample from 1300 cm (Shfd06134) was not completely reset prior to burial. Thus, the calculated age for this sample is underestimated. According to the laboratory report, the second sample (Shfd06135; 1500 cm depth) was well bleached and postdepositionally undisturbed allowing for reliable calculation of burial age. Obtained age for this sample was examined in context with the site stratigraphy and radiocarbon ages. The radiocarbon age for the sample from the depth 1487 cm confirmed fairly well the accuracy of the OSL age for the sample Shfd06135.

4.2. Sediment description and interpretation

4.2.1. Unit A (1505–1490 cm): ochre sand

The basal unit contains gravel-sized clasts in predominantly sandy sediments. The poorly sorted deposits of yellowish colour (2.5Y 4/2) are characterized by negligible TOC content. The basal

Table 1
AMS radiocarbon ages for the core in the Labe valley, the Krkonoše Mountains.

Unit	Depth (cm)	Material	Laboratory code	Radiocarbon age (^{14}C yr BP)	Calibrated age[a] (cal yr BP)	Median age[b] (cal yr BP)	Deposition rate (mm yr^{-1})
F	50	Peat	Erl-10098	2091 ± 42	2291–1948	2063	0.2
F	85	Peat	Erl-10099	2420 ± 43	2701–2348	2463	0.9
F	120	Peat	Erl-10100	2684 ± 43	2864–2744	2793	1.1
F	155	Peat	Erl-10101	2940 ± 46	3250–2958	3105	1.1
F	190	Peat	Erl-10102	3764 ± 46	4288–3981	4130	0.3
F	205	Peat	Erl-6295	4080 ± 49	4815–4435	4591	0.3
F	255	Peat	Erl-10103	4410 ± 49	5279–4859	4998	1.2
E2	290	Peat	Erl-10104	4746 ± 50	5589–5325	5491	0.7
E2	325	Peat	Erl-10105	4898 ± 49	5739–5488	5634	2.4
E2	355	Peat	Erl-6318	5024 ± 53	5904–5653	5778	2.0
E2	395	Plant tissue	Erl-10106	5438 ± 50	6386–6023	6238	0.9
E2	465	Plant tissue	Erl-10107	6171 ± 57	7247–6934	7072	0.8
E2	500	Plant tissue	Erl-10108	6555 ± 55	7571–7332	7467	0.9
E1	797	Plant tissue	Erl-7380	8216 ± 373	9445–8997	9194	1.7
D2	963	Plant tissue	Erl-6184	9572 ± 54	11133–10720	10931	1.0
D1	1040	Plant tissue	Erl-10245	10823 ± 373	13530–11508	12703	0.4
B	1487	Bulk sediment	Erl-11402	25709 ± 187	31210–30010[c]	30610	0.3

[a] Calibrated ages for the 95.4% confidence interval. Calibration with OxCal 4.4 using IntCal04 (Reimer et al., 2004).
[b] Calibrated age estimate based on the median of the probability distribution.
[c] Calibration with CalPal using CalPal-2007 Hulu (Weninger and Jöris, 2008).

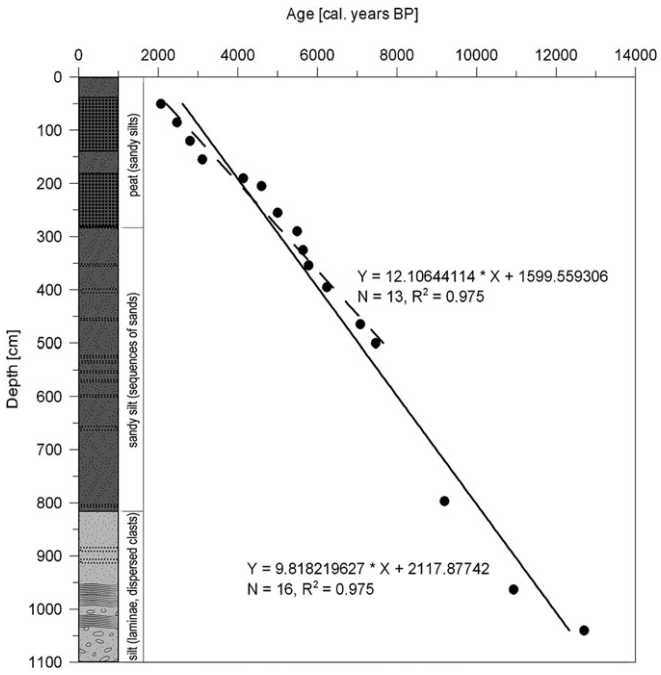

Fig. 2. Calibrated radiocarbon age versus depth of samples in the core. The solid line represents the best-fit line (least square regression) for the whole core, whereas the dashed line corresponds to dataset without the lowermost sample with high uncertainty of dating.

layer has sharp boundary with overlying unit (Fig. 3). Quartz grains are mostly angular with medium relief. Edge abrasion and upturned plates are the most common mechanical features, other frequent mechanical features are small conchoidal fractures, straight steps, imbricated blocks and straight grooves; silica precipitation occurs on the surface of 25% of the grains.

Unit A of inorganic sediments deposited in the Labe cirque at the end of MIS 3 which is consistent with the OSL age of 27,680 ± 1510 years of a sample from 1500 cm depth. The similarity of the basal sediments with higher lying sandy sections suggests that they originated during the period of increased fluvial runoff.

4.2.2. Unit B (1490–1466 cm): grey or light grey silt

Unit B consists of finely laminated clayey silt that overlies basal sands with dispersed clasts. The sequence contains couplets of layers that differ in thickness, composition and hue of grey colour (Gley1 5/1 10Y to 3/1 10Y). The TOC content ranges from 0.3% to 0.6%.

The unit of finely laminated sediments deposited at the end of MIS 3 which is consistent with the radiocarbon age of the uppermost lamina (31.2–30.0 cal ka BP). The presence of laminations indicates the development of limnic environment at the bottom of the cirque.

4.2.3. Unit C (1466–1245 cm): ochre diamict

Unit C contains diamict of yellowish colour (2.5Y 4/2) with consistently low TOC content (<0.6%). The unit consists of six sedimentary facies rich in sand (25–50%). Clast-rich diamict dominates the subunit C1 (1466–1340 cm) while clast-poor diamict prevails in subunit C2 (1340–1245 cm). The subunit C1 contains more subrounded quartz grains with high relief. Edge abrasion is typical for more than 50% of grains. Other frequent mechanical features are upturned plates, imbricated blocks and straight steps. Silica precipitation occurs on the surface of 25–40% of the grains, solution pits are frequent in the subunit C1 whereas adhering particles prevail in the subunit C2.

The gravel-bearing unit C deposited during the MIS 3–2 transition. Grain-size characteristics and particle shapes of the sedimentary unit are typical for tills (Fig. 4). The sequence deposited in the glacial environment due to glacier advances from the cirque to the upper Labe valley. The relics of lateral moraines on the eastern side of the cirque and terminal moraines in the trough document the extent and geomorphologic action of the valley glacier.

4.2.4. Unit D (1245–815 cm): grey to dark grey silt (with dispersed clasts)

Unit D is dominated by silt with sandy silt layers of dark to light grey colour (Gley1 4/1 10Y to 5/1 10Y). The light colour reflects the negligible content of organic material which is generally very low (<2.1%). Sandy silt dominates the subunit D1 (1245–995 cm) whereas silt with sand admixture is the main element of the subunit D2 (995–815 cm). Few sequences of muddy diamict occur within the subunit D1 showing the most prominent peak of the gravel fraction at depths 1108 and 1138 cm. Thin laminations dominate at depths 1029–1013, 990–972 and 969–953 cm. The only sandy silt sequence in the subunit D2 occurs between 868 and 855 cm. A notable feature of unit D is the slight upward decrease of clay particle content, accompanied by an increase in both sand and silt fractions (Fig. 5).

Quartz grains are mostly angular to subangular with predominantly medium to high relief. Edge abrasion is typical for half of the grains. Other frequent mechanical features are upturned plates, imbricated blocks, straight steps, large breakage blocks and arcuate steps (Fig. 6). Silica precipitation occurs on the surface of the grains in the subunit D1, adhering particles in the subunit D2. Micromorphological analyses of thin sections from depths 1180, 910 and 840 cm show fine lamination with positive gradation and laminae thickness of 0.1–2 mm. The lamination diminishes towards the top of the unit D and it is very indistinct in the thin section from the depth 840 cm. Coarse-grained fraction is composed by 60% of quartz grains, 30% of plagioclase grains and 10% of mica particles. Fine-grained matrix is monostriatic to spotted, partly also granostriatic with decomposed organic matter.

The unit of inorganic mud with dispersed clasts represents the limnic deposition. The proportional age (ca 11.9 cal ka BP) for the boundary (995 cm) of subunits D1 and D2 suggests that the deposition of the lower subunit terminated at the end of the Lateglacial period. The upper subunit was deposited during the early Holocene which is consistent with the radiocarbon data for the sample from 797 cm (9.4–9.0 cal ka BP). The varying colour and clast content together with a temporary increase of the TOC content in subunit D1 may reflect expansions and melting of the local glacier associated with climatic changes in the Lateglacial period. The laminated sequences can be attributed to the changing proglacial influx into the limnic environment arising in front of the retreating cirque glacier.

4.2.5. Unit E (815–280 cm): dark brown sandy silt

Unit E consists of poorly sorted sandy silt interleaved with discrete layers of sand. Massive sandy silt prevails in the subunit E1 (815–526 cm) whereas the subunit E2 (526–280 cm) is characterized by the frequent occurrence of discrete sandy layers. Abundant detritus give the silty deposit its dark brown colour (7.5 YR 3/1) whereas the colour of the sandy layers ranges from olive-grey (5 Y 4/1) to dark grey (10 YR 3/1). The layers associated with an influx of sand-sized sediment (up to 65%) have generally lower content of TOC (0.4–13.6%) than adjacent plant macroremain-rich silt (up to 21%). A remarkable feature of the TOC content is two-step increase at depth range of 815–530 and 517–295 cm.

Quartz grains are mostly angular with medium relief. Edge abrasion is typical for more than half of the grains. Other frequent

Table 2
Summary of OSL dating results.

Unit	Depth (cm)	Laboratory code	Palaeodose (Gy)	Dose rate (μGy yr^{-1})	Distribution of replicate data	Age (kyr)
C	1300	Shfd06134	33.93 ± 1.56	5441 ± 293	Multi-modal	6.240 ± 0.44
A	1500	Shfd06135	153.6 ± 2.81	5550 ± 286	Normal	27.680 ± 1.51

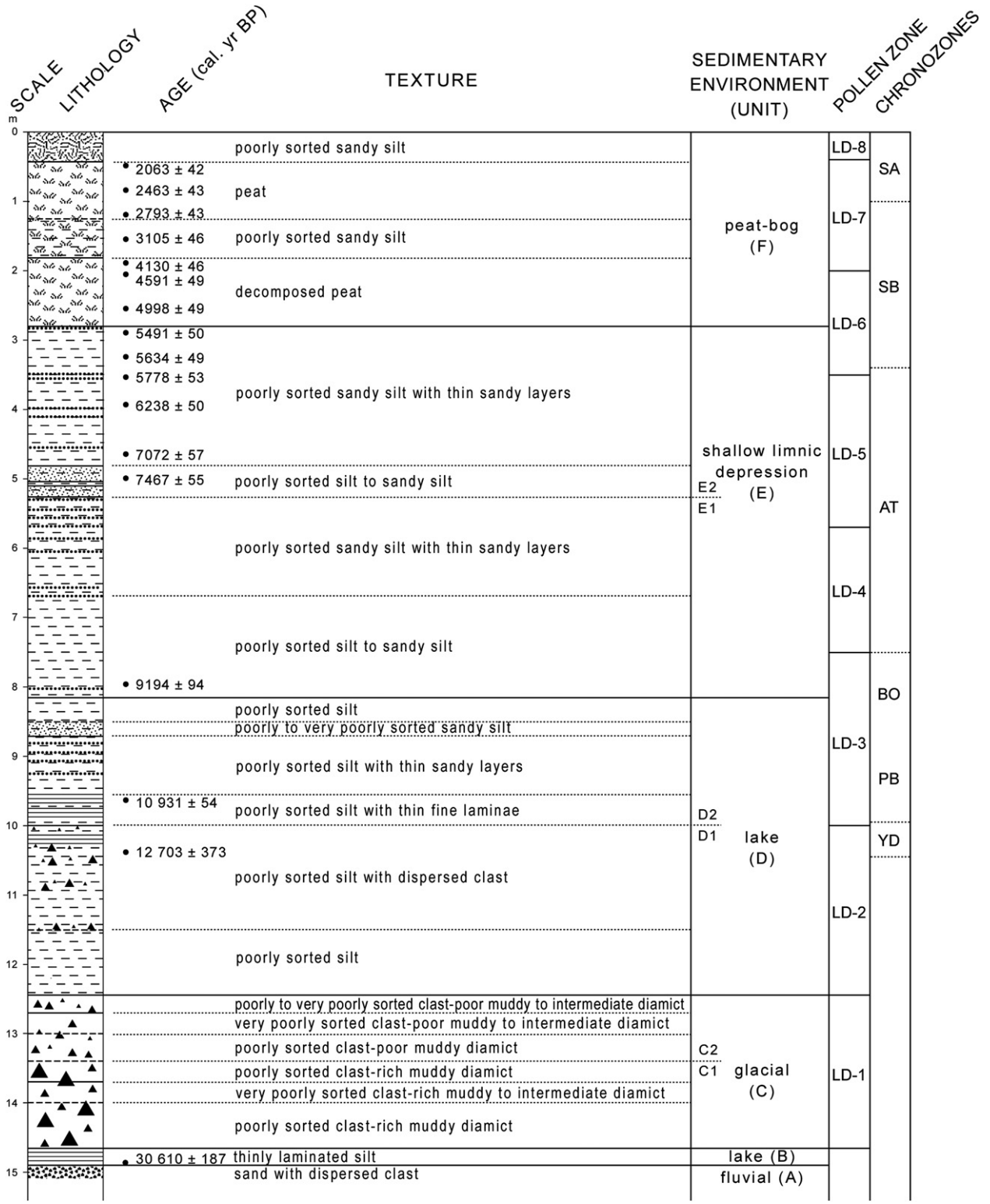

Fig. 3. Sedimentary log of the core from the Labe valley, depicting lithologic units and inferred sedimentary conditions.

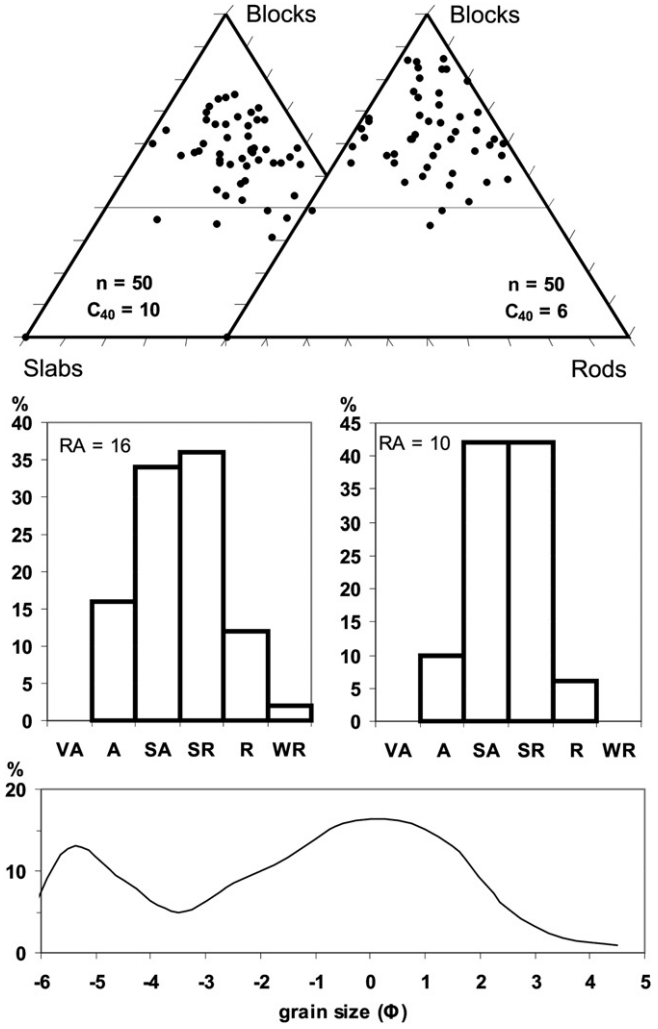

Fig. 4. Tri-plot diagrams, roundness histograms and particle size distribution for sediments from the depth 1387–1410 cm (left) and 1410–1426 cm (right). C_{40}, percentage of clasts with a c/a ratio of <0.4; VA, very angular; A, angular; SA, sub-angular; SR, subrounded; R, rounded; WR, well-rounded; RA, very angular and angular. Each sample consists of 50 clasts from the 2–4 mm and 4–8 mm fractions.

features are upturned plates, straight steps and imbricated blocks. Adhering particles are mostly more common than silica precipitation. Micromorphological analyses of thin sections from depths 805, 605 and 535 cm show mostly porphyritic and less commonly also massive microtexture. Grains compose coarse-grained fraction, sometimes plagioclase and mica particles are present. Monostriatic to spotty fine-grained matrix is made of decomposed organic matter, frustules and algae.

The deposition of the plant macroremain-rich unit started before ca 9.4–9.0 cal ka BP and terminated soon after 5.6–5.3 cal ka BP. The transition between subunits E1 and E2 (526 cm) corresponds to ca 7.6 cal ka BP. Sandy layers represent abrupt inputs of coarser sediment into the shallow limnic depression. Unimodal grain size distribution, low level of sorting and predominantly rounded to sub-rounded clast shape indicate sediment deposition by floods whereas abundant macroremains of terrestrial flora point to the derivation of sediment from lake catchment. Incursions of sandy deposits are attributed to intense precipitation events that caused widespread erosion of soil and vegetation in the upper Labe catchment area generating loose material susceptible to fluvial transport. The youngest events probably reflect climate changes in the Atlantic/Sub-Boreal transition (ca 340 cm).

4.2.6. Unit F (280–0 cm): dark brown organic-rich sandy silt and peat

The uppermost unit is formed by organic-rich sandy silt and peat. The dark brown (2.5 YR 2.5/2) lower part of this unit (280–182 cm) consists mainly of the decomposed plant macroremains. More consolidated organic material of brown colour (2.5 YR 3/1) is present between 182 and 147 cm depth. Its contact with the underlying section is sharp while the upper part transforms gradually into the light brown (2.5 YR 4/6) uppermost section (147–0 cm). Two sandy silt layers are present at 120–129 cm and 33–37 cm depths. The TOC content rises abruptly in the lowermost part of unit F reaching the maximum value (52%) in the profile. The TOC content remains high (>30%) up to the top of the profile, except for sequence between 190 and 140 cm where temporarily decreases (>8%) due to the fluvial influx of sandy silts. Quartz grains are predominantly angular with medium relief (Fig. 6). Only edge abrasion is commonly present as a mechanical surface feature. Adhering particles and silica precipitation represent frequent chemical features.

The organic-rich unit F deposited during the last 5350 years. The peat constitutes most of the upper part of the core and represents relatively slow deposition of organic and mineral matter throughout the late Holocene. Abrupt variations of grain-size distribution and TOC content in the middle section may reflect considerable climatic changes of the Sub-Boreal period (ca 340–100 cm). The silty layers in the upper part of the section can be attributed to floods.

4.3. Variations of TOC/TIC and magnetic susceptibility

The sediment core shows a three-step pattern in the TOC content throughout the Lateglacial and Holocene (Fig. 5). In the lower part of the core (up to 815 cm) the TOC content and its variation is very low. TOC is characterized by the content up to 1% in this section, exceeding slightly at the depth ranges 1055–1047, 949–944 and 920–890 cm. The middle part of the core (815–280 cm) shows apparently higher content and variability of TOC. The TOC content increases rapidly from 0.5% to >8% in the depth 815–785 cm. In the section up to 280 cm the TOC content varies mostly between 4% and 13%, with extreme values 0.5% and 21%. The upper part of the core (280–0 cm) is characterized by considerable higher and more variable TOC content ranging from 8% to 52%. The substantial growth in TOC content appears at the transition between the middle and upper section of the core (288–262 cm). Towards the top of the profile the TOC content gradually decreases to the present-day value of 40%, fluctuating abruptly in the depth range 180–140 cm. The TOC content tumbles below 8% due to fluvial influx and then increases back to values around 45% within this short section.

The TIC content is negligible (mostly below the detection limit of 0.05%) throughout the core profile with the exception of the lower part of the core (Fig. 5). In the lower part of the profile up to 1060 cm, the TIC content varies significantly ranging up to 0.8%. This section represents MIS 2 and Lateglacial period regarding radiocarbon age of the sample from 1040 cm (13.5–11.5 cal ka BP).

The magnetic susceptibility curve can be broadly divided into four parts (Fig. 5). There is a general increase in magnetic susceptibility from the beginning of MIS 2 until ca 18 cal ka BP (1175 cm) when χ culminates. This is followed by gradual decrease of magnetic susceptibility until ca 9.2 cal ka BP (800 cm), separated by two phases of increased χ: the first phase coincides with the Younger Dryas period (ca 1045–995 cm) and the second is centred at ca 9.5 cal ka BP (830 cm). A sharp transition to lower χ at the depth of 820–800 cm, terminating around 9.2 cal ka BP, marks the beginning of the central section of the profile which continues up to

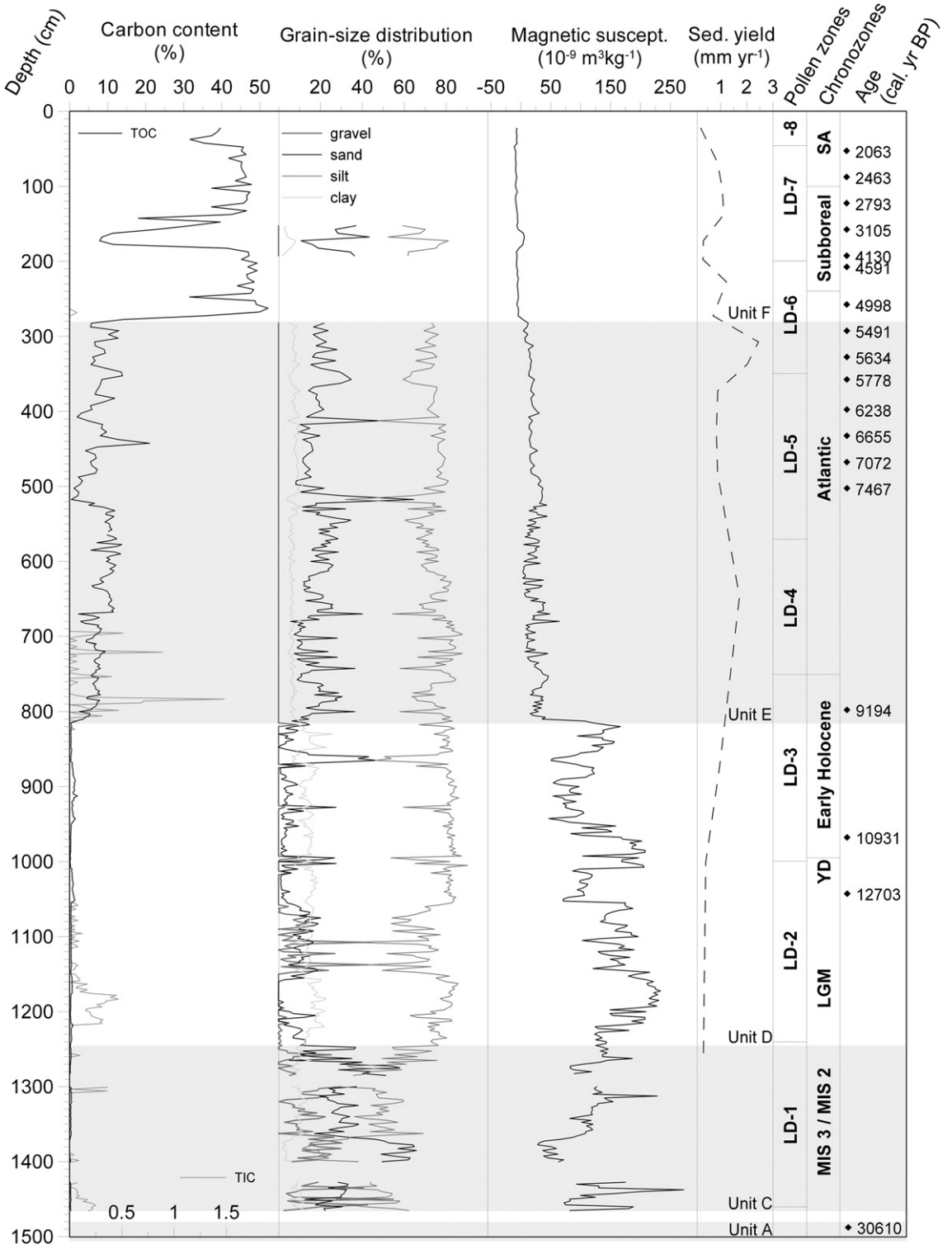

Fig. 5. The variations in sedimentation rate, magnetic susceptibility, grain-size and TOC/TIC content in the core. Note that TOC content (shown on the left-hand side) is geometrically similar and reversed to magnetic susceptibility curve.

ca 5.4 cal ka BP (280 cm). This section is characterized by series of minor oscillations of χ around a generally low value which may indicate warmer and more stable conditions. The last part of the profile begins with another drop of χ beginning at ca 5.4 cal ka BP. This is followed by a slight decrease of the magnetic susceptibility which was interrupted by temporary rise of χ centred at ca 3.7 cal ka BP (175 cm) due to fluvial influx as discussed above.

4.4. Pollen record

1460–1240 cm, LD-1. The occurrence of pollen in AP is continuous in the case of *Pinus sylvestris* t. and *Betula alba* t. (about 50% and 6% respectively; Fig. 7). *Pinus haploxylon* pollen (up to 5%) occurs almost continuously whereas solitary pollen grains belong to *Betula nana* t., *Juniperus*, *Alnus*, *Salix* and *Tilia*. The Poaceae pollen

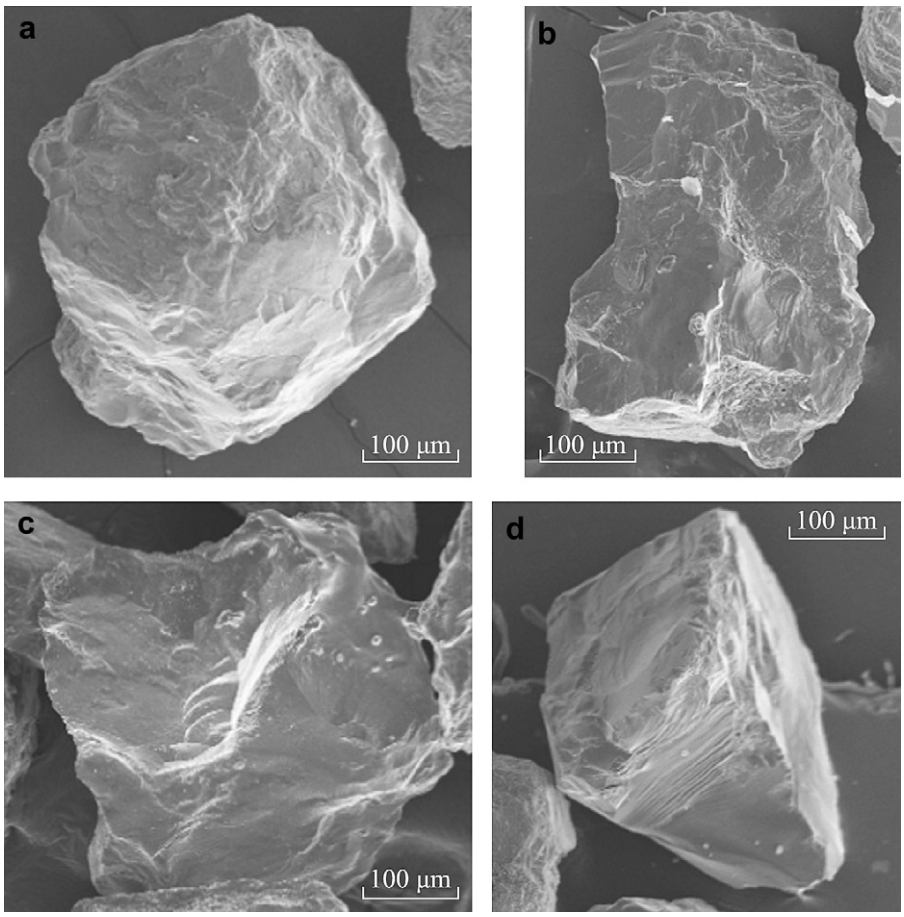

Fig. 6. SEM photographs of surface microtextures in samples. (a) Rounded grain with visible edge abrasion and V pits document aeolian transport history (depth 265 cm). (b) Angular grain with medium relief, upturned plates and small conchoidal texture (depth 265 cm). (c) Angular grain with higher relief. The large conchoidal fracture, upturned plates, imbricated blocks and edge abrasion document the glacial history (depth 990 cm). (d) Subrounded grain with high relief. The edge abrasion and striations point at the glacial history (depth 990 cm).

dominates in NAP along with *Artemisia*, Cyperaceae and Chenopodiaceae. Numerous are the palynomorphs of Pleistocene and Tertiary origin. *Botryococcus* sp. dominates algae among which the "old" types related to *Pediastrum kawraiskyi* were found (Fig. 8). The cysts of Dinoflagellata (class Dinophycae) are also present.

1240–1000 cm, LD-2. *Pinus sylvestris* t. (about 55%) prevails in AP. The occurrence of pollen of *Betula alba* t. (up to 10%), *B. nana* t. and *Salix* is continuous. Solitary pollen grains belong to *Corylus*, *Alnus* and *Picea*. The Poaceae pollen dominates in NAP. Pollen values of *Artemisia*, *Chenopodiaceae*, *Asteraceae* and *Thalictrum* are relatively high. The occurrence of *Helianthemum*, *Gentiana* t. and *Botrychium* is indicatively important. *Pediastrum* sp., *P. kawraiskyi* and *Botryococcus* sp. prevail among the coccal green algae.

1000–750 cm, LD-3. *Pinus sylvestris* t. (up to 65%) with *Betula alba* t. (about 15%) and *B. nana* t. (about 5%) dominate in AP. Closed pollen curves are formed by *Juniperus* and *Salix*, sporadic findings pertain to the pollen of *Ephedra*, *Pinus haploxylon* t., *Corylus*, *Ulmus*, *Alnus* and *Picea*. The occurrence of Poaceae, *Artemisia* and *Thalictrum* in NAP decreases. The occurrence of *Rumex acetosella-acetosa* and *Urtica* begins. The pollen curve of *Filipendula* and the occurrence of Polypodiaceae increases. The findings of *Pediastrum boryanum* var. *longicorne* colonies are also growing.

750–570 cm, LD-4. *Corylus* prevails with values up to 30% in AP. The pollen curve of *Betula alba* t. rises up to 20% at the beginning but then it sharply falls to nearly 5%. The pollen curves of *Ulmus*, *Quercus*, *and Tilia* are closing and the pollen values of *Alnus* and *Picea* sharply increase. The *Juniperus* pollen diminishes and the pollen curve of *Betula nana* t. shows a considerable decrease. Values of *Artemisia* and Poaceae considerably decrease in NAP; the occurrence of other herbs is qualitatively varied. The occurrence of spores of various ferns increases. The occurrence of coenobia of the genus *Pediastrum* terminates.

570–350 cm, LD-5. The values of *Corylus* vary in AP around 15% and those of *Pinus sylvestris* t. are only slightly lower. The occurrence of *Betula alba* t. pollen attains 10%. The proportion of *Ulmus*, *Quercus* and *Tilia* is even and together with a lower occurrence of *Fraxinus* and *Acer* the QM sum does not exceed 10%. The values of *Picea* pollen vary at about 15% and those of *Alnus* at about 10%. The spectrum of herbs is qualitatively varied but without the presence of any more important taxons. Spores of Polypodiaceae attain the highest values.

350–200 cm, LD-6. Pollen values of *Picea* attain their Holocene maximum (up to 40%), *Alnus* keeps steadily its 10%. The occurrence of *Pinus*, *Betula* and *Corylus* pollen decrease whereas the pollen curves of *Acer*, *Fagus*, *Abies* and *Carpinus* are closing. Stomata of *Picea* have been found. Some substantial changes appear in NAP. The occurrence of *Chamaenerium* and *Melampyrum* pollen comes to an end.

200–40 cm, LD-7. The proportion of *Fagus* increases from 1% to 17%, that of *Abies* from 1% to more than 22%. *Carpinus* forms a closed pollen curve with values in the range 1–6%. Pollen curve of *Picea* decreases from 35% to 10% and then increases again. A distinct decrease of pollen grains is shown by both *Corylus* and QM woods with the exception of *Quercus*. There are no substantial changes in NAP although the pollen grains of *Polygonum bistorta* t., *Petasites* t.,

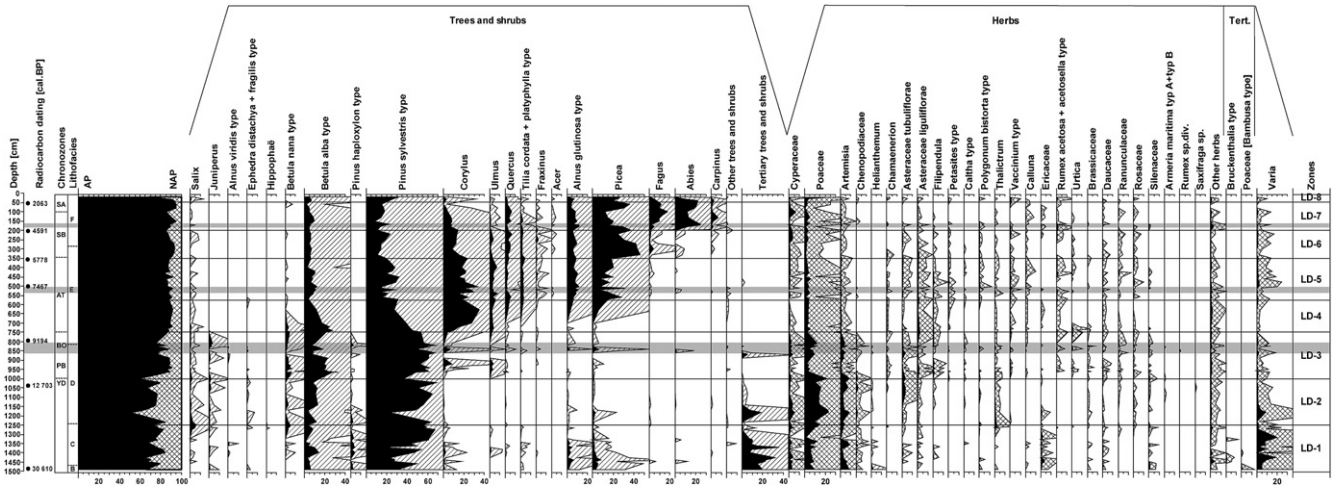

Fig. 7. Pollen diagram of the core for terrestrial vegetation with postulated cold periods. LD assemblage zone boundaries determined according the information content criterion for pollen taxa displaying curves, excepting Hydrophyta and non-pollen microfossils.

Filipendula and *Thalictrum* are disappearing. The occurrence of Asteraceae, Daucaceae and Polypodiaceae decreases while values of Cyperaceae slightly increase. The pollen of *Scheuchzeria* newly appears.

40–0 cm, LD-8. *Pinus* (about 30%) and *Picea* (25%) prevail in AP. Pollen curves of *Fagus* and *Abies* strongly decrease similarly to curves of other woody species. Only *Betula alba* t. and *Quercus* have higher pollen values. Distinct changes took place in NAP. Numerous pollen grains of *Secale*, *Triticum* t., *Avena* t., *Cerealia* sp., *Plantago lanceolata*, *Rumex acetosella* and *Cannabis* appear (not shown on Fig. 7). The proportion of Poaceae pollen abruptly increases.

5. Discussion

5.1. Sedimentation history in the upper Labe valley

The succession of sedimentary units in the core documents the development of environmental conditions in the upper Labe valley for last ca 30 ka. The sedimentary record of the core profile suggests that the end of MIS 3 is characterized by gradual environmental readjustment related to climatic change. The OSL dating and related laboratory analyses show that the sample from 1500 cm was fully reset prior to burial and that no post-depositional sediment disturbance has occurred. Thus, the sandy section at the depth of 1505–1490 cm was exposed to sunlight during the last transport event or after deposition. This suggests that the bottom of the cirque was not covered by glacier before the end of MIS 3. The overlying laminated sequence (1490–1466 cm) represents calm limnic sedimentation that terminated at ca 31.2–30.0 cal ka BP.

The sedimentary environment has changed towards full glacial conditions since the transition period between MIS 3 and MIS 2. A bimodal distribution of grain-size, blocky shape and intermediate roundness of clasts from unit C (1466–1245 cm) points at glacial transport of sediments associated with expanding cirque glacier. The glacial origin of sediments from this sequence is also supported by incomplete bleaching of the sample from 1300 cm which was deposited without exposure to the sunlight. Lack of radiocarbon data precludes detailed reconstruction of sedimentation dynamics. However, massive and homogenous structure of sedimentary unit suggests that the deposition was calm and regular until ca 13.5–11.5 cal ka BP (1040 cm). Mean rate of sedimentation was 0.3 mm yr^{-1} for this period.

Sedimentary conditions changed substantially in the cirque during the Termination I (ca 995 cm). The sedimentary section depositing since Younger Dryas (ca 1045–995 cm) to the early Holocene (ca 995–750 cm) is characteristic for ice-marginal and limnic environments. Deposition of thinly laminated clayey silts started around ca 12.4 cal ka BP (1029 cm) lasting until ca 10.8 cal ka BP (953 cm). The laminated sequences represent phases of sedimentation in a proglacial lake which arose at the margin of retreating cirque glacier. The presence of discrete sandy layers within the section points at phases of increased sedimentary input probably associated with oscillations of the glacier. Most of these sandy layers (including the most prominent one at the depth 860–868 cm) were deposited between ca 11.1 and 9.8 cal ka BP (972–860 cm), except for the layers at the depth range of 1007–1000 cm and 998–994 cm that could be correlated with the Younger Dryas period. The evidence from the described section thus supports the idea that glaciers existed in cirques until the early Holocene (Braucher et al., 2006). The observed sedimentation rates reflect variations of sedimentary conditions in the upper Labe catchment during the Termination I. The thinly laminated core sections represent "calm" periods with lower sedimentation rate (0.4 mm yr^{-1}) whereas the upper part with frequent sandy layers reflects periods of increased fluvial runoff with higher sediment yields (up to 1.0 mm yr^{-1}). A similar period of increased fluvial erosion and even more rapid sedimentation (as high as 2 mm yr^{-1}) during the Lateglacial–Holocene transition was described from the Ma^3y Staw Lake in the northern part of the Krkonoše Mts (Chmal and Traczyk, 1998).

The large amount of tertiary pollen types in the lowermost sequences indicates considerable input of material from the northern foreland of the Krkonoše Mts and long-distance transport from remote areas. Provenience of most palynomorphs and cysts (e.g. marine Dinoflagellata) suggests that they were redeposited from areas in front of Quaternary ice-sheet (southern Poland). These areas were affected by an intense wind action during cold and dry glacial periods serving as a source of material for deflation and aeolian transport (Jankovská, 2007). However, some of the Tertiary pollen admixture was transported from areas outside the Central Europe. Higher pollen production and treeless conditions in these areas favoured long-distance pollen transport (e.g. Bortenschlager, 1965; Fritz, 1976; Drescher-Schneider, 1993) which is active in recent conditions as well (Hladil et al., 2008).

Abrupt increase of clastic sediment input to the cirque floor beginning at around 9.4 cal ka BP (820 cm) delimits the period of rapid sedimentation dynamics. Significantly higher content of sand and sandy silts in the sequence overlying the lake section (D)

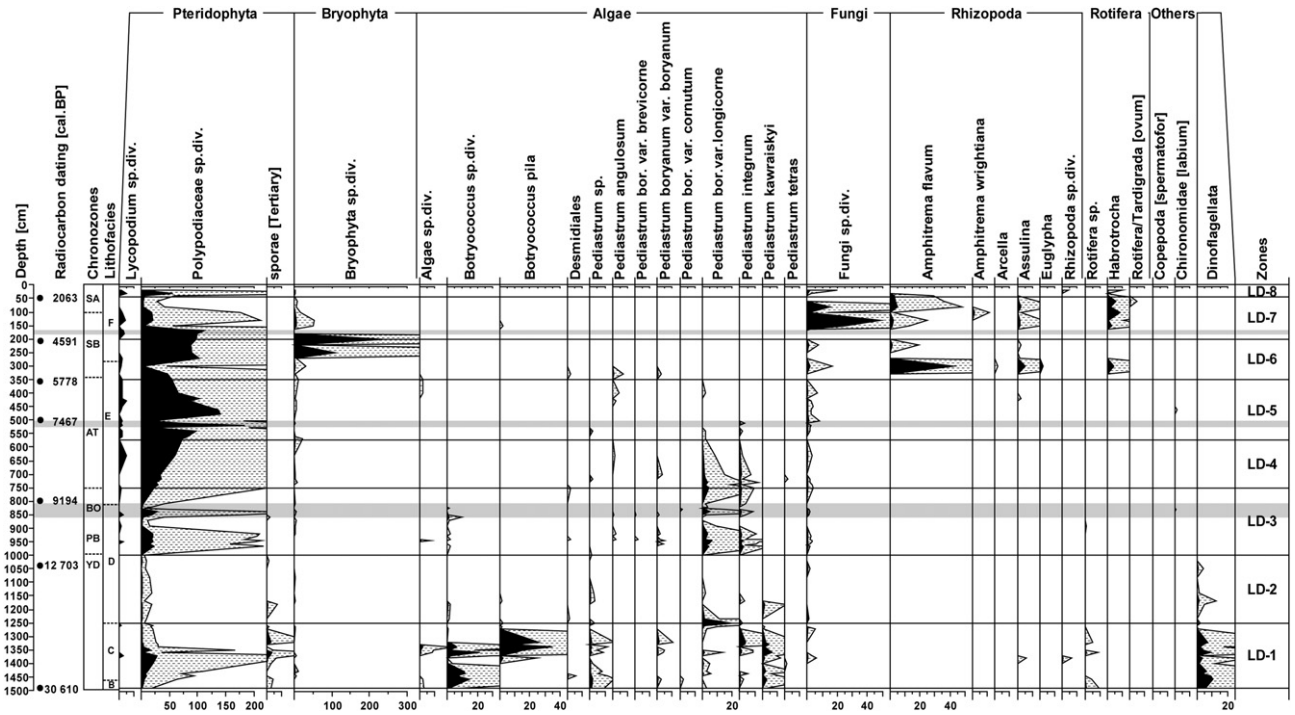

Fig. 8. Pollen diagram of the core for hygrophyte pollen and non-pollen microfossils. All taxa excluded from pollen sum. The postulated cold periods are indicated by grey stripe.

probably indicates the period of increased fluvial runoff associated with permafrost thawing in the lake's catchment, followed by progressive erosion in yet poorly vegetated landscape. The lower part of this sequence was formed during the paraglacial period. As Labe glacier retreated back from the cirque, freshly deglaciated cirque walls and moraines were the subject to rapid erosion. Oversteepened slopes and unstable glacial sediment delivered material into the cirque bottom directly or into fluvial system of the Labe River. Progressive landscape changes and dynamic morphological processes generated high sediment yields (up to 1.7 mm yr^{-1}) lasting until ca 7.5 cal ka BP (500 cm). The described section supports the hypothetical period of rapid deposition suggested by Chmal and Traczyk (1998), although it culminated a bit later compared to the concept for locations in the northern side of the mountains. The period of intense sedimentation coincides with increased activity of slope processes reported from mid-mountain areas in Central Europe (Czudek, 2005).

The subsequent period between ca 7.5 and 5.8 cal ka BP (500–355 cm) is characterized by predominantly regular sedimentation dynamics and moderate rates of sediment yield (as high as 0.9 mm yr^{-1}). Silty sediments prevailed within this period but the persistent high content of sandy fraction (with major peaks at the depth 520 and 410 cm) indicates that the accumulation area in the cirque floor gradually decreased. Interpretations of the sedimentological and palaeobotanical analyses suggest that the limnic sedimentary environment diminished during this period. After that, the sedimentary environment as well as the nature of source of organic matter changed rapidly from limnic to boggy. The described environmental conditions correspond with the phase of limited morphodynamics and relatively low rates of sedimentation determined for locations on the northern side of the mountains (Wicik, 1986; Chmal and Traczyk, 1998).

The period between ca 5.8 and 5.5 cal ka BP (355–290 cm) is characterized by a transition of limnic sedimentary environment to peat-bog. Following the termination of limnic environment an increasing amount of *Sphagnum* spores was deposited at the bottom of the cirque. Remarkable input of sands associated with increased fluvial runoff suggests that clastic sediment delivery from the surrounding terrain was rapid. Rapid environmental readjustment could be possibly related to the climatic change at the Atlantic/Sub-Boreal transition. Sediment yield (as high as 2.4 mm yr^{-1}) increased during this period up to highest values of the whole core profile. The observed rate of sedimentation is significantly higher compared to a value of 1.7 mm yr^{-1} reported by Chmal and Traczyk (1998) from $Ma^{3}y$ Staw Lake. However, the described period of the increased deposition and high rates of sedimentation coincides with the data published for sedimentary profiles in the upper Łomnica valley and the Śnieżne Kotły Cirques (Chmal and Traczyk, 1998).

Variable sedimentation conditions prevailed in the cirque between 5.5 and 2.8 cal ka BP (355–120 cm). Predominantly clastic sediments were transported from the catchment area by fluvial and slope processes but the deposition of organic sediments increased gradually. During almost 1000 years of peat accumulation, total organic content increased substantially from 16 to 95%. The sedimentation rate varied substantially (in the range 0.3 to 1.1 mm yr^{-1}) during this period due to intermittent inputs of coarser material to the cirque floor from the adjacent slopes. Increased sediment supply was probably facilitated by climate, oscillating between dry and more humid phases with intense precipitation events (Ložek, 2007). Rapid sedimentation was also reported from the northern slope of the mountains where slope and fluvial processes were attributed to climate cooling (Chmal and Traczyk, 1998). Peat sequences, accumulated at the end of this period, represent the last phase of rapid deposition in the core.

A low deposition rate controlled by the growth of the peat bog prevails within the last 2800 years of the core (120–0 cm). Depositional processes with predominantly organic accumulation were interrupted occasionally by seasonal flood events, debris-flows or avalanches, supplying clastic material into the bog. Calculated accumulation rates of peat vary between 0.2 and 1.1 mm yr^{-1}during this period. Peat formation was interrupted temporarily ca

1950 years ago (40–30 cm) when sandy silt section was deposited. Subsequently, peat started to accumulate again covering the bog by *Sphagnum* and *Polytrichum* mosses.

5.2. Climate and landscape changes since the Late Weichselian period

Magnetic susceptibility (χ) and a correlation of χ with published records (Patzelt, 1977; Haas et al., 1998; Davis et al., 2003) suggest that the climatic record of the study area is consistent with the Central European climatic pattern during the Late Weichselian and Holocene periods. Variations of magnetic susceptibility in the lower part of the core indicate cold conditions and highly variable climate in the study area connected mainly with direct glacial sedimentation of poorly sorted material or proglacial outwash into the limnic environment. The magnetic susceptibility of samples is unsteady throughout MIS 2 due to grain-size variability of glacigenic material. However, the general increasing trend until ca 18 cal ka BP (1175 cm) is seen, then χ values start to decrease (Fig. 5). Cold conditions during this period are witnessed by negligible TOC content and slight TIC presence in the diamict sequence of the core. Increased TIC content coincides with the culmination of the cold period, when increased aridity and intensive aeolian action increased soil dust input (Czudek, 2005). Pollen record reveals that vicinity of the site was generally sparsely vegetated with dominance of Poaceae and *Artemisia* species. The end of the described period was characterized by a significant wiggle in AP/NAP curve that reflects the Last Glacial Maximum. Nevertheless, the interpretation of the pollen record is somewhat uncertain since the sediment includes considerable proportion of reworked pollen, demonstrated by the presence of Tertiary palynomorphs (e.g. Ammann, 1989).

Magnetic susceptibility decreases gradually between ca 18 and 9.2 cal ka BP (1175–800 cm). The drop of χ after ca 13.5 cal ka BP (1060 cm) accompanied by a slight increase of TOC indicate a major temperature rise that probably correlates with the Allerød period. A sudden increase of magnetic susceptibility accompanied by a reset of the TOC content interrupted this warming, subsequently reaching the values comparable to glacial conditions. This shift to the cold climate is closely correlative with the Younger Dryas period (ca 1045–995 cm) associated with the revival of the periglacial environment in the Krkonoše Mts (Traczyk, 2004). The magnetic susceptibility record from this period shows three multisample oscillations that coincide with the major Younger Dryas glacier advances established in the northern Alps (e.g. Ivy-Ochs et al., 2006). The vegetation pattern coincides with unstable environmental conditions as well. A sudden increase in pollen proportion of trees was followed by an abrupt decrease of *Pinus sylvestris* type pollen linked to the considerable increase of both *Artemisia* and Poaceae pollen and the pollen of heliophilous shrubs (*Salix*, *Betula nana* type, *Ephedra distachya-fragilis* type) during the Younger Dryas event. The end of the Younger Dryas period was marked by substantial drop of the magnetic susceptibility followed by the increase of TOC content. The subsequent period indicates several climate deteriorations during the early Holocene (ca 995–750 cm). The presence of *Pediastrum boryanum* var. *longicorne* and *P. integrum* in samples indicates sedimentation in shallow cold oligothrophic lake during this time (Jankovská, 2004). The most prominent phase of χ increase interrupted the generally decreasing trend of magnetic susceptibility at ca 9.9 cal ka BP (865 cm) indicating climate cooling. This event is manifested in the significant decrease in AP/NAP rate and in related pollen changes. *Pinus* reached the highest values in the profile (48.7–70.7%) and together with *Betula* (8.5–19.5%) dominated the pollen spectra between ca 9.8 and 9.3 cal ka BP (860–810 cm). A short-term decrease of *Pinus* pollen percentage in the middle of this period was compensated by a significant increase of the *Picea* population which exceeded indicative value of the local presence (5% according to Huntley and Birks, 1983). All of these trees are characteristic of a rather cold climate (Zagwijn, 1996). Alpine treeline probably retreated to the lower elevations during this time (Treml et al., 2006). The cold event correlates with the Venediger phase in the Austrian Alps (Patzelt, 1977) and relevant oscillations reported from several sites in Central Europe (Haas et al., 1998; Roos-Barraclough et al., 2004; Joerin et al., 2006). Oscillations of magnetic susceptibility recorded in the core during the Lateglacial and early Holocene periods indicate alternations between warm and cold periods, respectively.

The sudden drop of magnetic susceptibility, coincident increase of the TOC and sand content clearly show a change by ca 9.4–9.2 cal ka BP (815–800 cm) indicating a shift in the depositional system related to a climatic change. In this period, the alpine treeline ecotone gradually shifted upslope above the cirque floor of Labský důl valley (Treml et al., 2006). Since then until 5.4 cal ka BP (280 cm), the magnetic susceptibility was relatively stable which probably corresponds to lower sensitivity of forest lakes to climatic events (e.g. Wick and Tinner, 1997). Besides a number of single-sample maxima and minima, a sequence with higher χ values is recorded in samples from ca 8.5–8.4 cal ka BP (680–655 cm). The grain-size curves show the notable change of sedimentation at ca 8.5 cal ka BP (675 cm) which is contemporaneous with minor cooling event in northern Switzerland (Haas et al., 1998) and thus probably climate-related. The small magnitude of change and a lack of clear trend are consistent with many palaeoclimate records from Central Europe (Davis et al., 2003). A minor change of magnetic susceptibility and TOC content in the core culminating at the depth of ca 630 cm represents a widely reported 8.2 cal ka BP cold event. This event is less obvious in samples if compared with similar records from Central and Western Europe (Wick and Tinner 1997; Kofler et al. 2005). The culmination of low χ values between ca 8.4–7.7 cal ka BP (650–530 cm) suggests that the Holocene Thermal Maximum started earlier than in sites located far to the west of Central Europe (e.g. Haas et al., 1998; Davis et al., 2003). TOC content raised well-above previous negligible values during the 9.4–9.2 cal ka BP (815–800 cm) and typical Holocene conditions were established. A notable increase in TOC content reflects increased delivery of organic matter from the catchment area. In addition, high sedimentation rates are documented as well (Fig. 5). It is assumed that the increased sedimentation of organic matter started soon after the deglaciation when the vegetation expanded into the landscape. The increase in TOC values corresponds with the forest expansion (increase in AP/NAP rate to 80%, abrupt decrease of pollen grains of heliophilous alpine shrub - *Betula nana* type) between 9.3 and 8.8 cal ka BP (810–730 cm). Subsequent variations in TOC content coincident with the magnetic susceptibility changes indicate warm climate and wet conditions until ca 7.7 cal ka BP (530 cm). After this period, the TOC dropped suddenly from >10% to 0.4%, indicating a local decline of forest vegetation (drop of pollen curves of *Pinus sylvestris* type, *Corylus*, *Betula alba* type, *Picea* succeeded by the increase of both Poaceae, *Artemisia* pollen and pollen of *Betula nana* type and *Ephedra distachya-fragilis* type). At that time the forest lake changed to fen.

The variations of magnetic susceptibility and frequent oscillations of the TOC with relatively high amplitudes (as high as 46%) in the upper part of the core suggest that the climate was variable between ca 7.6 and 5.2 cal ka BP (520–270 cm). Both the change of magnetic susceptibility and the drop of TOC around 7.7 cal ka BP point at a climatic deterioration that is terminated by an abrupt shift of the grain-size distribution. *Picea* became the dominant species between ca 7.7 and 7.5 cal ka BP (530–505 cm) with value of pollen percentage up to 32% following a continual regional

expansion of spruce population lasting since ca 8.6 cal ka BP. *Betula* population spread again during this period exceed 10% pollen percentage which is indicative value of the local presence according to Huntley and Birks (1983). The pollen data suggest the presence of open, light-demanding woodlands with *Lycopodium (Huperzia) selago* and *Selaginella* club-moss. The event is contemporaneous with the Frosnitz oscillation in the Austrian Alps (Patzelt, 1977) and relevant to the cold phases in Central Europe (e.g. Wick and Tinner, 1997; Haas et al., 1998). Other events reflecting low magnitude of change occurred around 7.0 and 6.4 cal ka BP (455 and 405 cm) and are coincident with the climate oscillation reported from the Eastern Alps (Kofler et al., 2005) and Lake Seedorf in Switzerland (Magny et al., 2003). Described conditions are consistent with highly unstable climate reported by Ložek (2007) from the whole Bohemian Massif. Magnetic susceptibility decreases slightly during this period indicating a tenuous warming trend. Observed conditions contradict the generally accepted view of substantial cooling during the Upper Atlantic and Sub-Boreal periods (Chmal and Traczyk, 1998; Rybníčková and Rybníček, 2001) and supports the hypothesis of considerably warmer climates during the beginning of the Sub-Boreal (Skrzypek et al., 2009). The rapid increase in TOC between ca 5.4 and 5.2 cal ka BP (285–270 cm) can by attributed to the beginning of peat accumulation in the cirque. TOC rises at the same sequence where the *Picea* pollen exceeds 40% (Fig. 7). It is argued that *Picea* expanded in the central part of the Krkonoše Mts during the Sub-Boreal period when there was a climatic shift to a more humid climate (Jankovská, 2007). The humid conditions favoured mire expansion, higher organic production and input of carbon into the sedimentary basin. According to the position of the core within the peat bog in the scarce forest during the Sub-Boreal period, the TOC content indicates rather local environmental changes than regional climatic events.

Starting in 5.2 cal ka BP (270 cm), the climatic conditions tend to be more stable than in preceding periods according to variations of magnetic susceptibility and TOC content in samples. This is consistent with reconstructions of palaeotemperatures in the northern foreland of the Swiss Alps reported by Heiri et al. (2003). A gradually decreasing trend in the TOC content during the last 5000 years corresponds to a generally declining temperature indicated by several studies in the Krkonoše Mts (Speranza et al., 2000; Jankovská, 2004) and other sites in Central Europe (Davis et al., 2003). The only prominent event interrupted the Sub-Boreal period at ca 4.0–3.3 cal ka BP (185–160 cm). Abrupt drop of the TOC content (from 47% to 8%) and its subsequent increase back to values prior to the oscillation probably reflect temporary decline in temperature and/or humidity. A notable increase of magnetic susceptibility coincides with the shift of TOC and with minor changes of the pollen data. The percentages of *Pinus*, *Quercus* and *Abies* pollen increased reaching critical values for local presence (Huntley and Birks, 1983). The regional expansion of species resistant to cold was simultaneous with local decrease of *Fagus* and *Carpinus* which are typical for temperate climate. These changes correspond to $\delta^{13}C$ variations in peat from adjacent Jizerské hory Mts (Skrzypek et al., 2009). In addition, the event coincides with the glacier advances in the Alps (Patzelt, 1977; Leeman and Niessen, 1994) and with corresponding cold event that has been observed in various sedimentary records on the Swiss Plateau (Tinner et al., 1996; Haas et al., 1998; Heiri et al., 2003). The above-mentioned sequence of the profile is followed by a peat section with a slight decrease of the magnetic susceptibility which indicates a return to warmer conditions. A notable increase of temperature at ca 2.5 cal ka BP (90 cm) was determined from $\delta^{13}C$ variations in peat (Engel et al., in press). This short-term warming episode represents the commonly accepted Sub-Boreal/Sub-Atlantic transition (Birks and Birks, 1980).

6. Conclusions

1. The succession of sedimentary units in the lower part of the core documents the development of the glacier in the upper Labe valley during the Late Weichselian. The sedimentary record suggests that the bottom of the cirque was ice-free at the end of MIS 3 and that the glaciation developed during MIS 2. Thinly laminated silts at the depth range of 1029–1013 cm point at the retreat of the local glacier from the upper Labe trough into the cirque during the termination of Lateglacial period which is consistent with the radiocarbon age of 13.5–11.5 cal ka BP for a sample from the depth of 1040 cm. Subsequent interruption of the laminated sediment formation suggests that the glacier probably advanced and filled the cirque floor again. Following the restoration of limnic environment, laminated silts were deposited at the beginning of the Holocene (until ca 10.8 cal ka BP).

2. Two phases of increased sedimentation occurred in the upper Labe valley during the last 10 ka. The first phase started at the beginning of the Holocene and culminated during the period from about 9.2 to 7.5 cal ka BP. The sediment yield was as high as 1.7 mm yr^{-1} during this period. The second period (5.8–5.5 cal ka BP) of rapid sedimentation reflects the Atlantic/Sub-Boreal transition. The rate of sedimentation (2.4 mm yr^{-1}) was highest during the beginning of the Sub-Boreal compared to the entire record.

3. On the basis of pollen analysis, magnetic susceptibility and TOC content in samples, palaeoclimatic patterns were reconstructed at the Labe cirque for the last ca 30 ka. Highly variable climate prevailed during MIS 2 with cold conditions culminating at ca 18 cal ka BP. Rapid changes in magnetic susceptibility and TOC in the samples reflect cold conditions and highly variable climate at the end of the Lateglacial period. The most prominent climatic events during the Lateglacial were the major warming followed by the Younger Dryas deterioration. Palaeoclimatic conditions in the early Holocene times fluctuated strongly whereas since 5.1 cal ka BP was more stable. Besides a number of less pronounced climatic events, three periods with lower temperatures are apparent during the Holocene: an abrupt shift to a cooler climate around 9.8–9.3 cal ka BP and prominent climate deteriorations at ca 7.7–7.5 cal ka BP and 4.0–3.3 cal ka BP.

4. The results indicate that the most rapid changes in TOC occur due to the changes in the extent of adjoining mires. The study confirms that a change to a warmer and more humid climate can increase the TOC levels in sedimentary basin.

5. The vicinity of the sample site was covered by sparse, treeless vegetation until the end of Younger Dryas event. Later the site was invaded by tree species (*Pinus*, *Betula*) and treeline ecocline shifted upwards. Early Holocene climatic events were expressed in treeline oscillations at 9.8–9.3 cal ka BP and probably also at 7.7–7.5 cal ka BP. The local treeline consequently ascended high above the study site and the composition of the surrounding forest changed to *Picea* dominated growths in the Middle Holocene followed by *Abies–Fagus* growths established after ca 4.2 cal ka BP.

6. Investigated sedimentary records in the Labe cirque with limnic sediments are of high importance since only few lakes have risen in the Krkonoše Mts during the deglaciation period. Succession of fine-grained mineral deposits, followed by organic sediments and peat corresponds with the sedimentary records from other sites in the Krkonoše Mts. It is thus suggested that presented results are valid on regional scale giving evidence for similar landscape evolution within the whole Krkonoše Mts.

Acknowledgements

The study was funded by the Czech Science Foundation (project 205/06/0587) and by the Czech Ministry of Education, Youth and

Sports (project MSM 0021620831). The authors would like to acknowledge Krkonoše N.P. Administration for providing permission to work in the region. Finally, the authors would like to thank Josef Víšek for measuring magnetic susceptibility and grain-size parameters, Andrzej Traczyk for research assistance, and Miroslav Šobr and Martin Margold for fieldwork support.

References

Ammann, B., 1989. Response times in bio and isotope stratigraphies to Late-Glacial climatic shifts an example from lake deposits. Eclogae Geologicae Helvetiae 82, 183–190.

Bieroński, J., Chmal, H., Czerwiński, J., Klementowski, J., Traczyk, A., 1992. Współczesna denudacja w górskich zlewniach Karkonoszy. Prace Geograficzne 155, 151–169.

Birks, H.J.B., Birks, H.H., 1980. Quaternary Palaeoecology. Edward Arnold, London.

Bortenschlager, S., 1965. Funde afrikanischer Pollen in den Alpen. Naturwissenschaften 52 (24), 663–664.

Braucher, R., Kalvoda, J., Bourlès, D.L., Brown, E., Engel, Z., Mercier, J.-L., 2006. Late Pleistocene deglaciation in the Vosges and the Krkonoše Mountains: correlation of cosmogenic ^{10}Be exposure ages. Geografický časopis 58, 1–12.

Bronk Ramsey, C., 2001. Development of the radiocarbon calibration program OxCal. Radiocarbon 43, 355–363.

Carr, S.J., Engel, Z., Kalvoda, J., Parker, A., 2007. Towards a revised model of Late Quaternary mountain glaciation in the Krkonoše Mountains, Czech Republic. In: Goudie, A.S., Kalvoda, J. (Eds.), Geomorphological Variations. P3K, Praha, pp. 253–268.

Chmal, H., Traczyk, A., 1993. Plejstoceńskie lodowce gruzowe w Karkonoszach. Czasopismo Geograficzne 64, 253–263.

Chmal, H., Traczyk, A., 1998. Postglacjalny rozwój rzeźby Karkonoszy i Gór Izerskich w świetle analizy osadów rzecznych, jeziornych i stokowych. In: Sarosiek, J., Štursa, J. (Eds.), Geoekologiczne problemy Karkonoszy. Acarus, Poznań, pp. 81–87.

Czudek, T., 2005. Vývoj reliéfu České Republiky v kvartéru. Moravské zemské muzeum, Brno.

Davis, B.A.S., Brewer, S., Stevenson, A.C., Guiot, J., Contributors, Data, 2003. The temperature of Europe during the Holocene reconstructed from pollen data. Quaternary Science Reviews 22, 1701–1716.

Drescher-Schneider, R., 1993. Funde nordafrikanischer Pollen in spät-und postglazialen Sedimenten am Südrand der Alpen. Festschrift Zoller. Dissertationes Botanicae 196, 415–425.

Dumanowski, B., Jahn, A., Szczepankiewicz, S., 1962. The Holocene of Lower Silesia in the light of results of the first radiocarbon dating. Bulletin de l'Académie Polonaise des Sciences, Série des sciences geologiques et geographicues 10, 47–52.

Engel, Z., 1997. Současný stav poznatků o pleistocenním zalednění české části Krkonoš. Geografie - Sborník ČGS 102, 288–302.

Engel, Z., 2007. Late Pleistocene glaciations in the Krkonoše Mountains. In: Goudie, A.S., Kalvoda, J. (Eds.), Geomorphological Variations. P3K, Praha, pp. 269–286.

Engel, Z., Treml, V., Krížek, M., Jankovská, V., 2004. Lateglacial/Holocene sedimentary record from the Labe source area, the Krkonoše Mts. Acta Universitatis Carolinae - Geographica 39 (1), 95–109.

Engel, Z., Skrzypek, G., Paul, D., Drzewicki, W., Nývlt, D. Sediment lithology and stable isotope composition of organic matter in a core from a cirque in the Krkonoše Mountains, Czech Republic. Journal of Paleolimnology. in press, doi:10.1007/s10933-009-9356-1.

Evans, M.E., Heller, F., 2003. Environmental Magnetism. Principles and Applications of Enviromagnetics. Academic Press, San Diego.

Folk, R.L., 1954. The distinction between grain size and mineral composition in sedimentary rock nomenclature. Journal of Geology 62, 344–359.

Fritz, A., 1976. Pollen im Sahara-Staub. Carinthia II. 166 (86), 173–174.

Gale, S., Hoare, P., 1991. Quaternary Sediments: Petrographic Methods for the Study of Unlithified Rocks. Belhaven, London.

Graham, D.J., Midgley, N.G., 2000. Graphical representation of particle shape using triangular diagrams: an Excel spreadsheet method. Earth Surface Processes and Landforms 25, 1473–1477.

Grimm, E.C., 1991. TILIA and TILIA GRAPH software. Illiniois State Museum.

Haas, J.N., Rischoz, I., Tinner, W., Wick, L., 1998. Synchronous Holocene climatic oscillations recorded on the Swiss Plateau and at the timberline in the Alps. The Holocene 8, 301–309.

Heiri, O., Lotter, A.F., Hausmann, S., Kienast, F., 2003. A chironomid-based Holocene summer air temperature reconstruction from the Swiss Alps. The Holocene 13, 477–484.

Hladil, J., Strnad, L., Šálek, M., Jankovská, V., Šimandl, P., Schwarz, J., Smolík, J., Lisá, L., Koptíková, L., Rohovec, J., Böhmová, V., Langrová, A., Kociánová, M., Melichar, R., Adamovič, J., 2008. An anomalous atmospheric dust deposition event over Central Europe, 24 March 2007, and fingerprinting of the SE Ukrainian source. Bulletin of Geosciences 83 (2), 175–206.

Huntley, B., Birks, H.J.B., 1983. An atlas of past and present pollen maps for Europe: 0–13 000 years ago. Cambridge University Press, Cambridge.

Hüttemann, H., Bortenschlager, S., 1987. Beiträge zur Vegetationsgeschichte Tirols VI: Reisengebirge, Hohe Tatra–Zillertal, Kuhtai. Berichte des Naturwissenschaftlich-Medizinischen Vereins in Innsbruck 74, 81–112.

Ivy-Ochs, S., Kerschner, H., Kubik, P.W., Schlüchter, C., 2006. Glacier response in the European Alps to Heinrich event 1 cooling: the Gschnitz stadial. Journal of Quaternary Science 21, 115–130.

Jahn, A., 1977. The permafrost active layer in the Sudety mountains during the last glaciation. Quaestiones Geographicae 43, 29–43.

Jankovská, V., 2004. Krkonoše vdobě poledové: vegetace a krajina. Opera Corcontica 41, 111–123.

Jankovská, V., 2007. Giant Mountains and pollenanalytical research: New results and interesting palaeobotanical findings. Opera Corcontica 44, 207–222.

Joerin, U.E., Stocker, T.F., Schlüchter, C., 2006. Multicentury glacier fluctuations in the Swiss Alps during the Holocene. The Holocene 16, 697–704.

Kofler, W., Krapf, V., Oberhuber, W., Bortenschlager, S., 2005. Vegetation responses to the 8200 cal. BP cold event and to long-term climatic changes in the Eastern Alps: possible influence of solar activity and North Atlantic freshwater pulses. The Holocene 15, 779–788.

Leeman, A., Niessen, F., 1994. Holocene glacial activity and climatic variations in the Swiss Alps: reconstructing a continuous record from proglacial lake sediments. The Holocene 4, 259–268.

Ložek, V., 2007. Zrcadlo minulosti. Česká a slovenská krajina v kvartéru. Dokořán, Praha.

Magny, M., Begeot, C., Guiot, J., Marguet, A., Billaud, Y., 2003. Reconstruction and palaeoclimatic interpretation of mid-Holocene vegetation and lake-level changes at Saint-Jorioz, lake Annecy, French Pre-Alps. The Holocene 13, 265–275.

Mahaney, W.C., 2002. Atlas of sand grain surface textures and applications. University Press, Oxford.

Mangerud, J., Andersen, S.T., Berglund, B.E., Donner, J.J., 1974. Quaternary stratigraphy of Norden, a proposal for terminology and classification. Boreas 3, 85–104.

Mazur, S., Aleksandrowski, P., 2001. The Tepla(?)/Saxothuringian suture in the Karkonosze-Izera massif, western Sudetes, central European Variscides. International Journal of Earth Sciences 90, 341–360.

Mercier, J.-L., Kalvoda, J., Bourlès, D.L., Braucher, R., Engel, Z., 2000. Preliminary results of ^{10}Be dating of glacial landscape in the Giant Mountains. Acta Universitatis Carolinae. Geographica 35 (Suppl.), 157–170.

Metelka, L., Mrkvica, Z., Halásová, O., 2007. Podnebí. In: Flousek, J., Hartmanová, O., Štursa, J., Potocki, J. (Eds.), Krkonoše. Baset, Praha, pp. 147–154.

Migoń, P., 1999. The role of preglacial relief in the development of mountain glaciation in the Sudetes, with the special reference to the Karkonosze Mountains. Zeitschrift für Geomorphologie N.F., Suppl.-Bd. 113, 33–44.

Moncrieff, A.C.M., 1989. Classification of poorly-sorted sedimentary rocks. Sedimentary Geology 65, 191–194.

Moore, P.D., Webb, J.A., Collinson, M.E., 1991. Pollen Analysis. Blackwell, Oxford.

Munsell Soil Color Chart, 2000. GretagMacbeth, New Windsor.

Patzelt, G., 1977. Der zeitliche Ablauf und das Ausmass postglazialer Klimaschwankungen in den Alpen. In: Frenzel, B. (Ed.), Dendrochronologie und postglaziale Klimaschwankungen in Europa. Steiner, Wiesbaden, pp. 248–259.

Reimer, P.J., Baillie, M.G.L., Bard, E., Bayliss, A., Beck, J.W.J., Bertrand, C.J.H., Blackwell, P.G., Buck, C.E., Burr, G.S., Cutler, K.B., Damon, P.E., Edwards, R.L., Fairbanks, R.G., Friedrich, M., Guilderson, T.P., Hogg, A.G., Hughen, K.A., Kromer, B., McCormac, G., Manning, S., Bronk Ramsey, C., Reimer, R.W., Remmele, S., Southon, J.R., Stuiver, M., Talamo, S., Taylor, F.W., van der Plicht, J., Weyhenmeyer, C.E., 2004. IntCal04 Terrestrial Radiocarbon Age Calibration, 0–26 cal kyr BP. Radiocarbon 46, 1029–1058.

Roos-Barraclough, F., van der Knaap, W.O., van Leeuwen, J.F.N., Shotyk, W., 2004. A Late-glacial and Holocene record of climatic change from a Swiss peat humification profile. The Holocene 14, 7–19.

Rybníčková, E., Rybníček, K., 2001. Vegetation development in the Czech Republic in the last 15 000 years. In: Neuhäuselová, Z., et al. (Eds.), Braun-Blanquetia, 30. Potential natural vegetation of the Czech Republic, pp. 12–15.

Skrzypek, G., Baranowska-Kącka, A., Keller-Sikora, A., Jędrysek, M.O., 2009. Analogous trends in pollen percentages and carbon stable isotope composition of Holocene peat—possible interpretation for paleoclimate studies. Review of Palaeobotany and Palynology 156, 507–518.

Speranza, A., van der Plicht, J., van Geel, B., 2000. Improving the time control of the Subboreal/Subatlantic transition in a Czech peat sequence by ^{14}C wiggle-matching. Quaternary Science Reviews 19, 1589–1604.

Stoops, G. (Ed.), 2003. Guidelines for Analysis and Description of Soil and Regolith Thin Sections. Soil Science Society of America, Madison, WI.

Stuiver, M., Polach, H.A., 1977. Discussion: reporting of ^{14}C data. Radiocarbon 19, 355–363.

Telford, R.J., Heegaard, E., Birks, H.J.B., 2004. The intercept is a poor estimate of a calibrated radiocarbon age. The Holocene 14, 296–298.

Tinner, W., Ammann, B., Germann, P., 1996. Treeline fluctuations recorded for 12,500 years by soil profiles, pollen and plant macrofossils in the Central Swiss Alps. Arctic and Alpine Research 28, 131–147.

Traczyk, A., 2004. Late Pleistocene evolution of periglacial and glacial relief in the Karkonosze Mountains: new hypotheses and research perspectives. Acta Universitatis Carolinae, Geographica 39 (1), 59–72.

Treml, V., Jankovská, V., Petr, L., 2006. Holocene timberline fluctuations in the mid-mountains of Central Europe. Fennia 184, 107–119.

Weninger, B., Jöris, O., 2008. A ^{14}C age calibration curve for the last 60 ka: the Greenland-Hulu U/Th timescale and its impact on understanding the Middle to Upper Paleolithic transition in Western Eurasia. Journal of Human Evolution 55, 772–781.

Weninger, B., Jöris, O., Danzeglocke, U., 2007. CalPal-2007. Cologne Radiocarbon Calibration & Palaeoclimate Research Package. http://www.calpal.de/ accessed 2007-07-05.
Wicik, B., 1986. Asynchronicznosc procesow wietrzenia i sedymentacji w zbiornikach jeziornych Tatr i Karkonoszy w postglacjale. Przeglad Geograficzny 58, 809–823.
Wick, L., Tinner, W., 1997. Vegetation changes and timberline fluctuations in the central Alps as indicators of Holocene climatic oscillations. Arctic and Alpine Research 29, 445–458.
Zagwijn, W., 1996. An analysis of Eemian climate in western and central Europe. Quaternary Science Reviews 15, 451–469.